

Supplementary Information

Methylthiophene terminated D- π -D molecular semiconductor as multifunctional interfacial material for high performance perovskite solar cells

Hao Zhang,^a Yuhua Mao,^a Jie Xu,^b Shanshan Li,^a Fusheng Guo,^a Lingyu Zhu,^a Jianli Wang^a and Yongzhen Wu*^b*

^a State Key Laboratory Breeding Base of Green Chemistry-Synthesis Technology, College of Chemical Engineering, Zhejiang University of Technology, Hangzhou 310014, PR China. E-mail: wangjl@zjut.edu.cn

^b School of Chemistry and Molecular Engineering, East China University of Science and Technology, Shanghai 200237, China. E-mail: wu.yongzhen@ecust.edu.cn

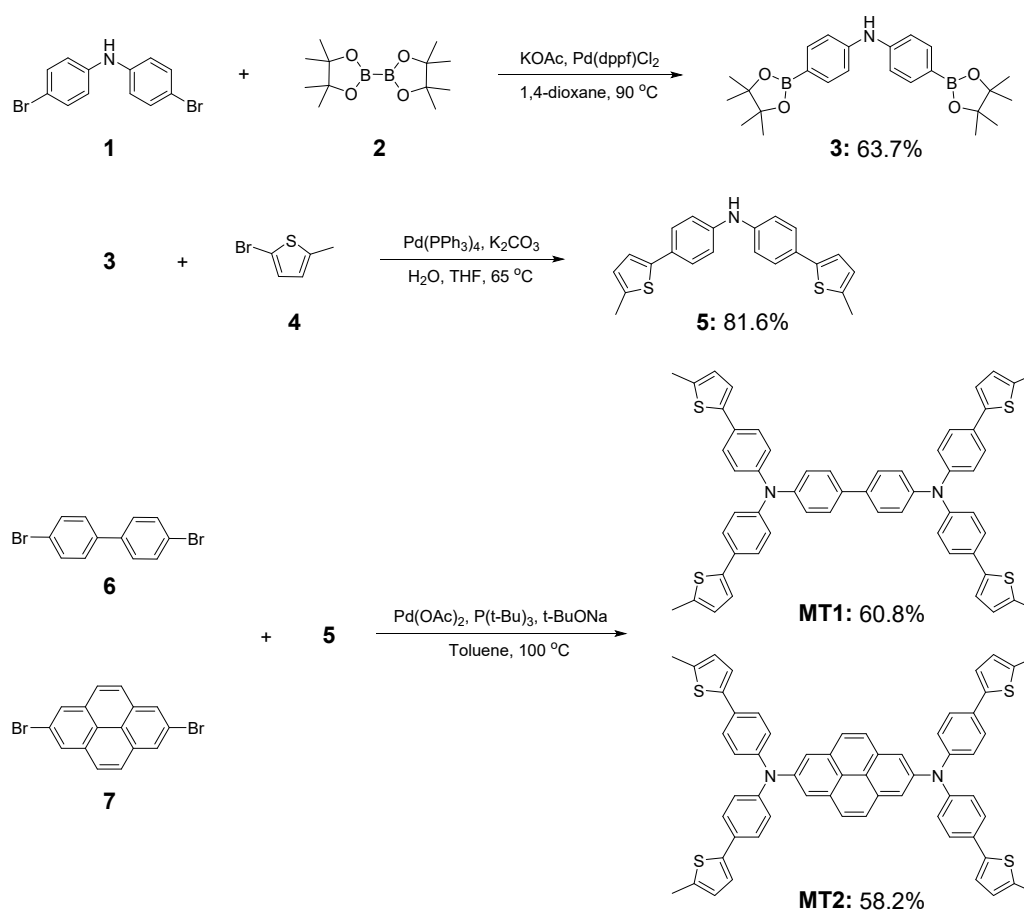
Contents

1. Materials and reagents	2
2. Synthetic routes	2
3. Perovskite solar cells fabrication	5
4. Characterization and measurements	5
5. ¹H, ¹³C NMR and HRMS characterizations	8
6. DFT/TDDFT calculation of MT1 and MT2.....	13
7. Thermal properties of MT1 and MT2.....	15
8. XPS, SEM, AFM, PL and TRPL results.....	16
9. The <i>J-V</i> curve, IPCE spectra and integrated current curves	18
10. The operation stability test at elevated temperature	19
11. Time-resolved photoluminescence decay fitting parameters	20
12. Thickness measurement results	20
13. References	20

1. Materials and reagents

All chemicals and solvents used for synthesis were of reagent grade and were obtained from Energy Chemical, Shanghai Titan Scientific Co., Ltd. and so on. The materials for perovskite solar cells fabrication were used as received, including Lead (II) Iodide (PbI₂, Kanto Chemical Co., Inc, Japan), Methylamine Hydroiodide (MAI, >98%, TCI). The SnO₂ colloid precursor was obtained from Alfa Aesar (tin(IV) oxide, 15% in H₂O colloidal dispersion), and the nanoparticles were diluted by deionized water to 2.67% before use. Other materials and solvents used for perovskite solar cell fabrication were purchased from Sigma-Aldrich. For NMR characterization, tetramethylsilane is used as external reference and the peak at 0.07 ppm nearby is due to the impurity of the deuterated solvent (CDCl₃).

2. Synthetic routes



Scheme S1. Synthetic route of MT1 and MT2.

Synthesis of intermediate 3. Intermediate **3** was synthesized by a similar way to the method in reference 1. In a three-neck round-bottom flask, compound **1** (2.0 g, 6.13 mmol), **2** (6.2 g, 24.47 mmol), KOAc (3.6 g, 36.7 mmol) were added to 60 mL dry 1,4-dioxane. The system was purged with argon for 15 min, and Pd(dppf)Cl₂ (0.90 g, 1.23 mmol) was added to the solution. Then, the reaction mixture was heated up to 90 °C, and stirred for 10 h under argon atmosphere. After cooling to the room temperature, the solvent was evaporated and the residue was dissolved in CH₂Cl₂ and washed with brine. The organic phases were combined together, dried over anhydrous Na₂SO₄, and purified by column chromatography on silica gel (petroleum ether : ethyl acetate = 8 : 1) to give 2.28 g white solid, affording intermediate **3** in 63.7% yield. ¹H NMR (400 MHz, CDCl₃, δ, ppm): 7.72 (d, *J* = 8.24 Hz, 4 H), 7.08 (d, *J* = 8.32 Hz, 4 H), 6.05 (s, 1 H), 1.33 (s, 24 H).

Synthesis of intermediate 5. In a Schlenk tube, compound **3** (2.0 g, 4.75 mmol) was dissolved in THF (30 mL), Pd(PPh₃)₄ (0.28 g, 0.24 mmol), K₂CO₃ (3.28 g, 23.77 mmol), and 10 mL water were added and the solution was degased and filled with nitrogen for three times. Then, compound **4** (1.4 mL, 11.30 mmol) was injected into the tube. The mixed solution was heated at 65 °C under nitrogen atmosphere and stirred for 12 h. After cooling to the room temperature, the organic phase were separated with a separatory funnel. Then, the solvent (THF) was evaporated and the residue was dissolved in CH₂Cl₂ and washed with brine. The organic phases were combined together, dried over anhydrous Na₂SO₄, and purified by column chromatography on silica gel (petroleum ether : CH₂Cl₂ = 2 : 1) to give a off white solid in 81.6% yield (1.40 g, 3.87 mmol). ¹H NMR (400 MHz, CDCl₃, δ, ppm): 7.46 (d, *J* = 8.56 Hz, 4 H), 7.06 (d, *J* = 8.60 Hz, 4 H), 7.01 (d, *J* = 3.48 Hz, 2 H), 6.70 (d, *J* = 3.48 Hz, 2 H), 5.80 (s, 1 H), 2.50 (s, 6 H). ¹³C NMR (150 MHz, CDCl₃, δ, ppm): 142.19, 126.74, 126.21, 121.80, 119.26, 118.16, 115.85, 15.59. HRMS-ESI (*m/z*): [M + H]⁺ Calcd. For (C₂₂H₂₀NS₂), 362.1037, found: 362.1037.

Synthesis of MT 1. In a three-neck round-bottom flask, compound **5** (1.00 g, 2.77 mmol), **6** (0.41 g, 1.32 mmol), Pd(OAc)₂ (12 mg, 0.05 mmol) and t-BuONa (0.53 g, 5.45 mmol) were added to 20 mL dry toluene. After stirring under nitrogen atmosphere at room temperature for 10 min, P(t-Bu)₃ (0.61 mL, 0.25 mmol) was injected into the mixture. Then, the reaction mixture was heated up to 100 °C and stirred for 12 h. After cooling to room temperature, the solvent was evaporated and the residue was dissolved in CH₂Cl₂ and washed with brine. The organic phases were combined together, dried over anhydrous Na₂SO₄, filtered and evaporated under reduced pressure. The crude product was purified by column chromatography on silica gel (petroleum ether : CH₂Cl₂ = 1 : 2) and recrystallized from a mixed solution of dichloromethane and methanol to afford **MT1** as a dark green powder in 60.8% yield (626 mg, 0.80 mmol). ¹H NMR (400 MHz, CDCl₃, δ, ppm): 7.44-7.49 (m, 12 H), 7.17 (d, *J* = 8.36 Hz, 4 H), 7.12 (d, *J* = 8.44 Hz, 8 H), 7.03 (d, *J* = 3.40 Hz, 4 H), 6.71 (d, *J* = 2.60 Hz, 4 H), 2.50 (s, 12 H). ¹³C NMR (150 MHz, CDCl₃, δ, ppm): 146.46, 141.88, 139.00, 135.24, 129.58, 127.59, 126.51, 126.32, 124.54, 124.45, 122.33, 15.62. HRMS-ESI (*m/z*): [M + H]⁺ Calcd. For (C₅₆H₄₅N₂S₄), 873.2466, found: 873.2466.

Synthesis of MT 2. The **MT2** was synthesized in a similar manner to that for **MT1**, affording a light yellow powder in 58.2% yield (611 mg, 0.66 mmol). ¹H NMR (400 MHz, CDCl₃, δ, ppm): 7.89 (s, 4 H), 7.81 (s, 4 H), 7.47 (d, *J* = 8.64 Hz, 8 H), 7.18 (d, *J* = 8.56 Hz, 8 H), 7.05 (d, *J* = 3.40 Hz, 4 H), 6.72 (d, *J* = 3.44 Hz, 4 H), 2.51 (s, 12 H). ¹³C NMR (150 MHz, THF-d₈, δ, ppm): 147.75, 145.84, 142.42, 139.18, 132.92, 130.48, 128.03, 126.92, 125.02, 122.91, 121.89, 15.11. HRMS-ESI (*m/z*): [M + H]⁺ Calcd. For (C₆₀H₄₅N₂S₄), 921.2466, found: 921.2452.

3. Perovskite solar cells fabrication

The ITO glass substrates were rinsed with deionized water and ethanol, then washed in isopropanol and acetone with sonication for 10 min, respectively, and finally cleaned with ultraviolet ozone treatment for 20 min. For the fabrication of SnO₂ nanoparticles films, the diluted SnO₂ nanoparticles solution (2.67%) was spin coated onto the ITO substrate in ambient air at a speed of 3,000 r.p.m. for 30s, and then annealed at 150 °C for 30 min. Perovskite films were deposited onto the SnO₂ nanoparticle layer by one step “anti-solvent” method from a precursor solution containing PbI₂ (1.26 M) and MAI (1.20 M) dissolved in anhydrous mixed solvent DMF: DMSO (5:1, volume ratio). The substrates were then annealed at 100 °C for 10 minutes and cooled down for a few minutes. For SIMs treatment, the corresponding molecular semiconductors in chloroform solution (1 mg/mL) was spin coated onto the perovskite films at 3,000 r.p.m for 30 s followed by thermal annealing at 60 °C for 5 min. The HTM was deposited by spin-coating (3000 rpm for 30 s) a solution of *spiro*-OMeTAD (60 mM) in chlorobenzene, with *tert*-butylpyridine (TBP, 330 mol%), and tris(bis(trifluoromethylsulfon-yl)imide) (Li-TFSI, 50 mol%) as additives. Finally, 80 nm thick film of Au was thermally evaporated under high vacuum on top of the hole transporting layer.

4. Characterization and measurements

All the perovskite films prepared for characterization and measurements was treated by the same process to that of the perovskite solar cells fabrication. The UV-vis absorption spectra were recorded with a Varian Cary 100 spectrophotometer. The cyclic voltammograms were measured by using an Ivium State.h electrochemical workstation in a three-electrode cell. The working electrode was a glassy carbon electrode, used in conjunction with a Pt wire counter electrode and a saturated calomel reference electrode. An amount of 0.1 M tetrabutylammonium hexafluorophosphate (TBAPF₆) was used as the supporting electrolyte in CH₂Cl₂. The ferrocene/ferrocenium (Fc/Fc⁺) redox couple was used as an external potential

reference. The scan rate was 100 mV/s. Thermal gravity (TG) analyses were performed with a heating rate of 10 °C min⁻¹ from 25 up to 850 °C under nitrogen atmosphere by a TG 209 F3 Tarsus (Netzsch, Germany). The differential scanning calorimetry (DSC) was performed on Netzsch DSC 200 F3 instrument and the DSC data were recorded in the temperature range from 20 to 300 °C at a heating rate of 10 °C min⁻¹. X-ray photoelectron spectroscopy (XPS) spectra were obtained with an ESCALab220i-XL electron spectrometer from VG Scientific using 300 W Al_{Kα} radiation and deconvoluted using XPS PEAK41 software. Scanning electron microscopy (SEM) measurements were performed with Zeiss G500. Atomic force microscopy (AFM) analysis was performed by Bruker Edge Dimension instrument. Steady state photoluminescence (PL) spectra were measured with a Horiba Fluoromax-4 fluorescence spectrometer. PL lifetimes were determined with the single photon counting technique by means of Edinburgh FLS980 spectrometer. X-ray diffraction (XRD) measurement was performed on a Rigaku D/max 2550 VB/PC apparatus. The contact angle water on the surface of perovskite films were measured by Dataphysics OCA-20 sessile drop method. To estimate the thicknesses of interface layers, MT1 and MT2 were deposited on smooth silicon substrates and measured by spectroscopic ellipsometry (M-2000, J. A. Woollam) with an incident angle of 70° and a light spot size of 360 × 360 μm. The coating thickness was calculated by the Cauchy model ($A_n = 1.45$, $B_n = 0.01$, and $C_n = 0$). Each thickness measurement was performed on three different positions to obtain an average value.

Photocurrent density–voltage ($J-V$) curves of devices were measured by Keithley 2400 Source meter Instruments under standard AM 1.5 simulated solar irradiation (WXS-155S-10) with using a black metal mask, with aperture area of 0.09 cm². The IPCE spectra were measured by Newport-74125 system (Newport Instruments). Transient photovoltage and photocurrent decay were recorded on a digital oscilloscope (DPO2012B, Tektronix. Inc) and the light pulse was provided by NL 100 nitrogen laser (Stanford Research System. Inc).

The dark current of hole only devices were recorded by Keithley 2400 Source meter Instruments. For hole mobility measurement, the results were fitted to a space charge limited form, based on equation S1:

$$J = 9\mu\varepsilon_0\varepsilon_r V^2 / 8d^3 \quad (\text{S1})$$

where J is the current density, μ is the hole mobility, ε_0 is the vacuum permittivity (8.85×10^{-12} F m⁻¹), ε_r is the dielectric constant of the material (normally taken to approach 3 for organic semiconductors), V is the applied bias, d is the film thickness of the active layer determined through AFM measurement. For defect density measurement, the n_{trap} values were calculated from equation S2:

$$n_{\text{trap}} = 2\varepsilon\varepsilon_0 V_{\text{TFL}} / eL^2 \quad (\text{S2})$$

Where ε is the relative dielectric constant of perovskite (32 F/m), L is the thickness of the perovskite film, e is the elementary charge of the electron ($e = 1.6 \times 10^{-19}$ C), and ε_0 is the vacuum permittivity.

5. ^1H , ^{13}C NMR and HRMS characterizations

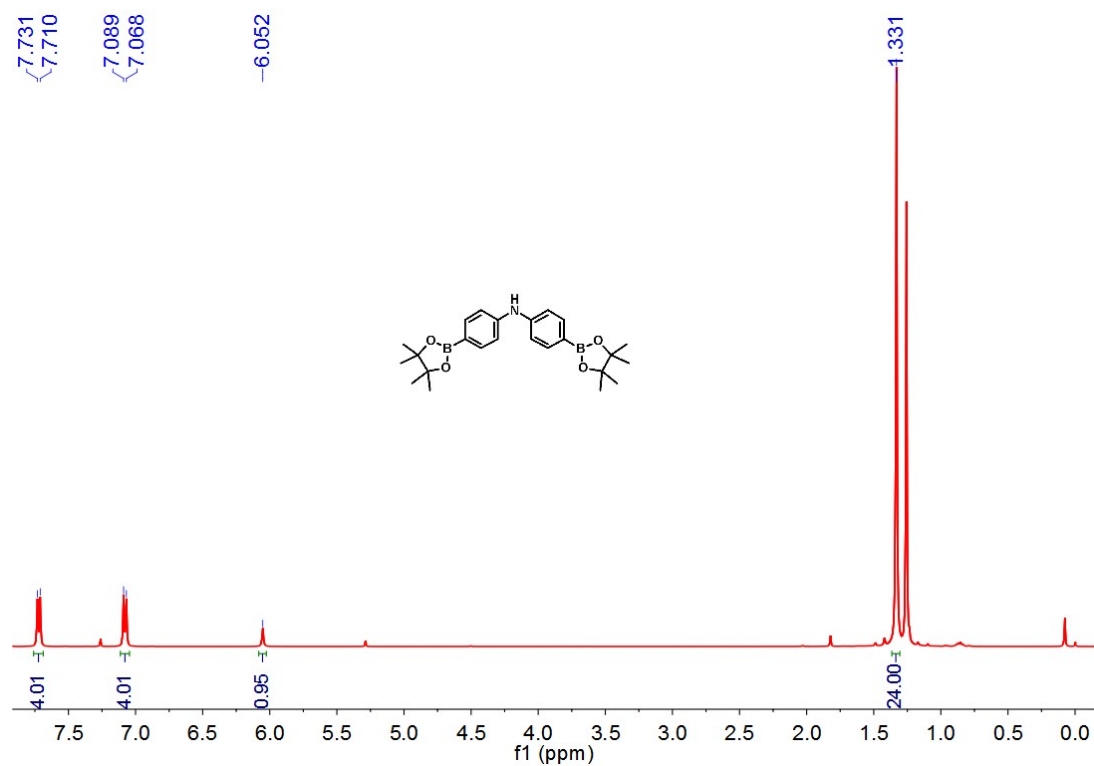


Fig. S1 ^1H NMR of intermediate **3** recorded in CDCl_3 .

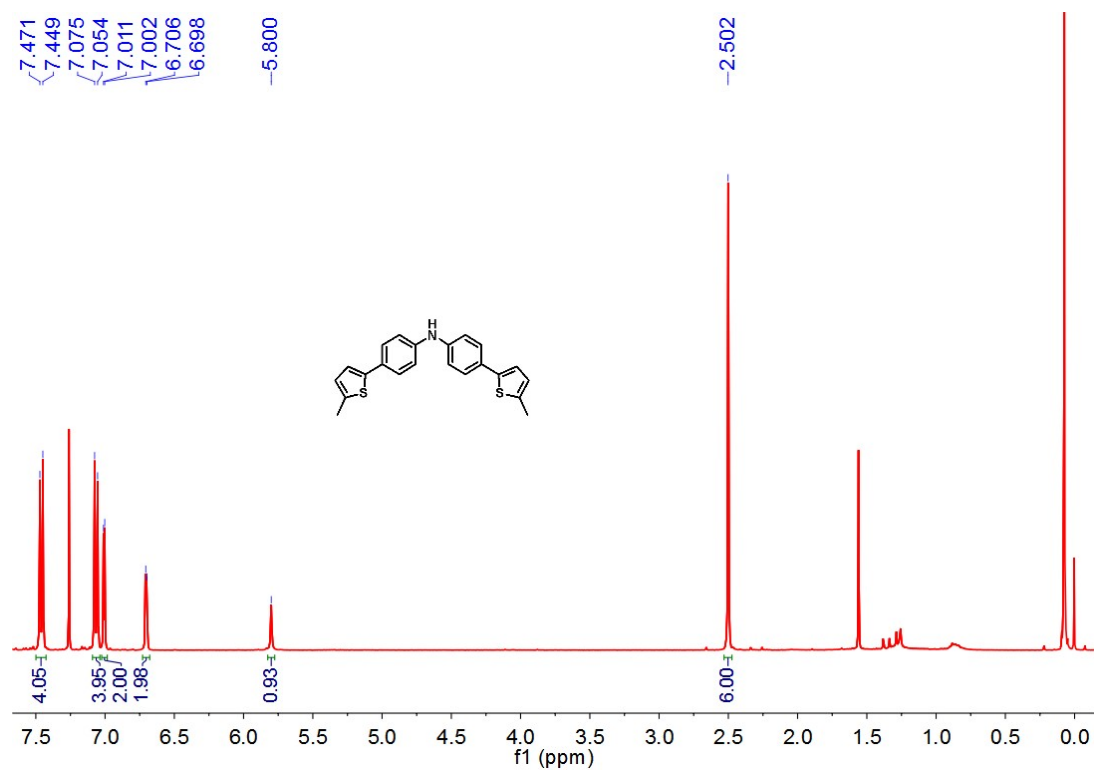


Fig. S2 ^1H NMR of intermediate **5** recorded in CDCl_3 .

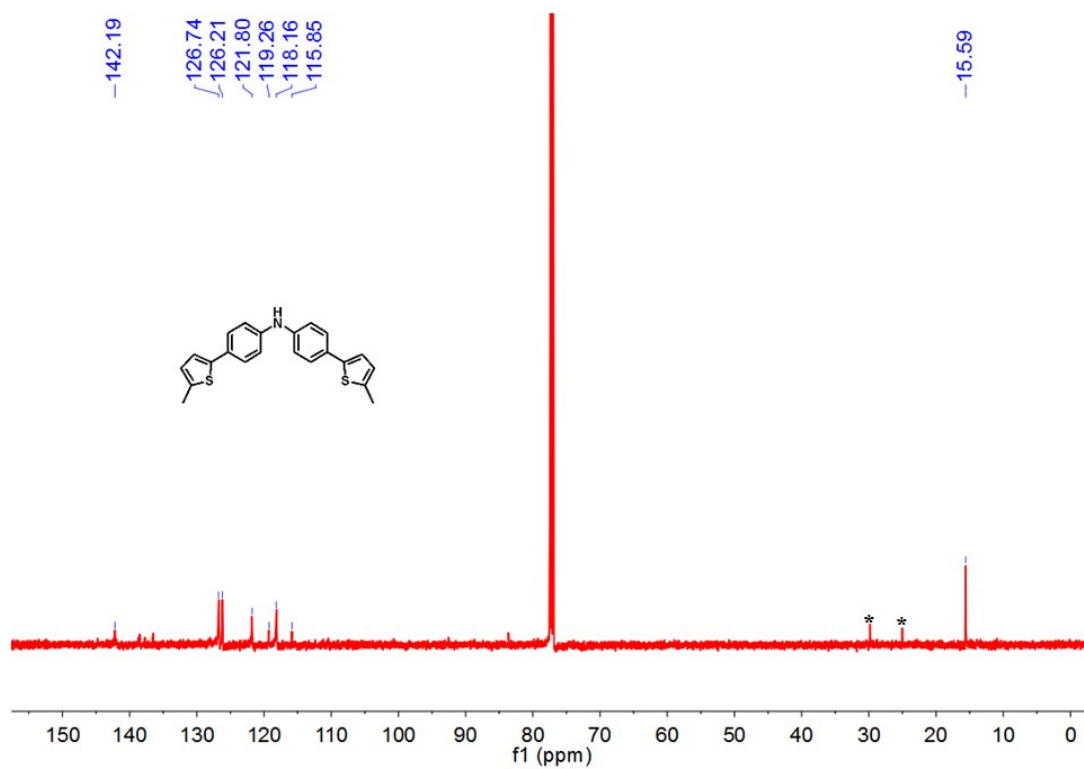


Fig. S3 ^{13}C NMR of intermediate **5** recorded in CDCl_3 . * represents some impurities.

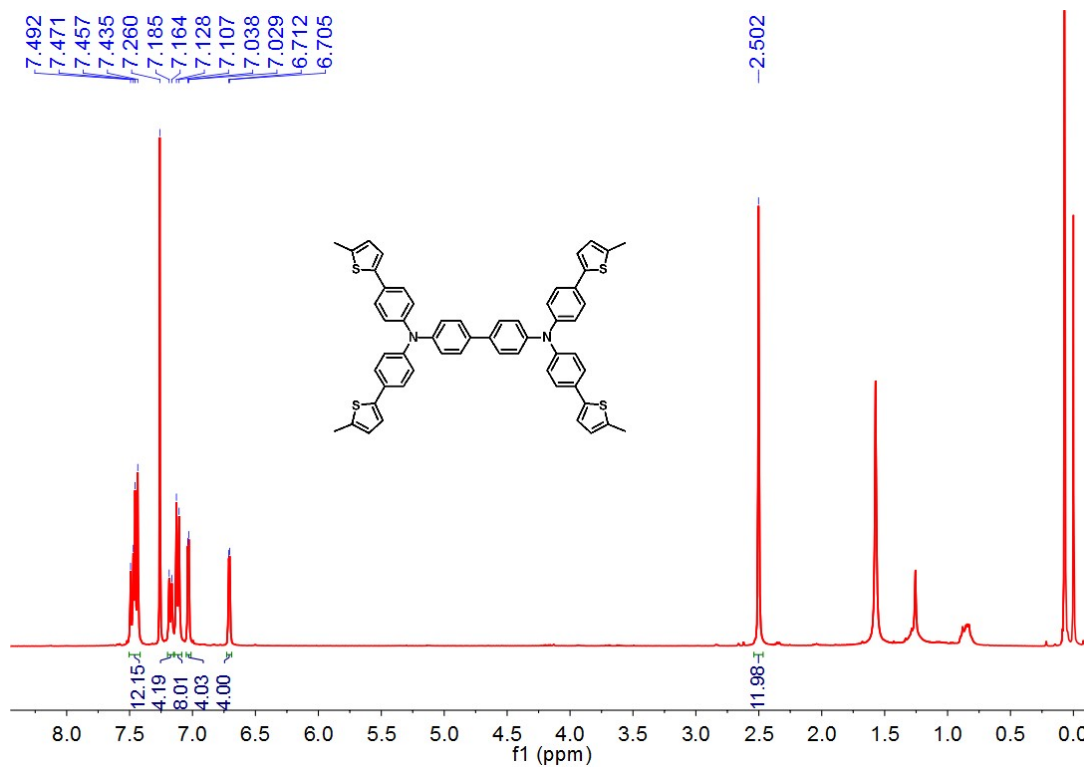


Fig. S4 ^1H NMR of **MT1** recorded in CDCl_3 .

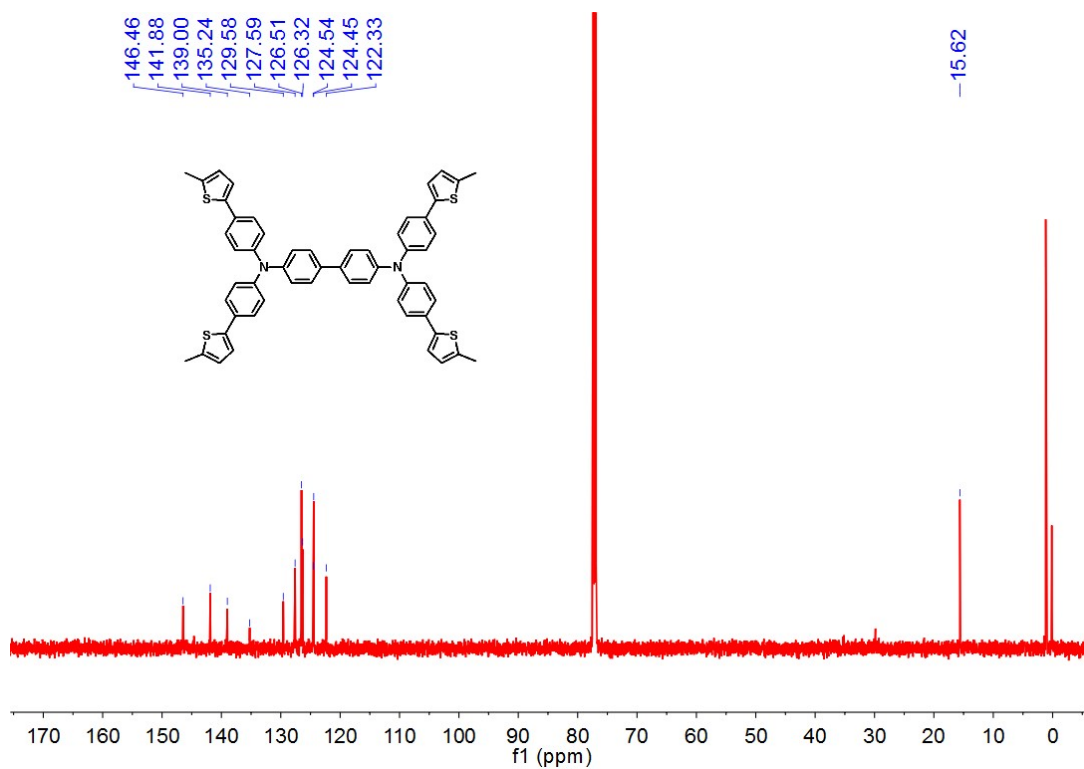


Fig. S5 ¹³C NMR of MT1 recorded in CDCl₃.

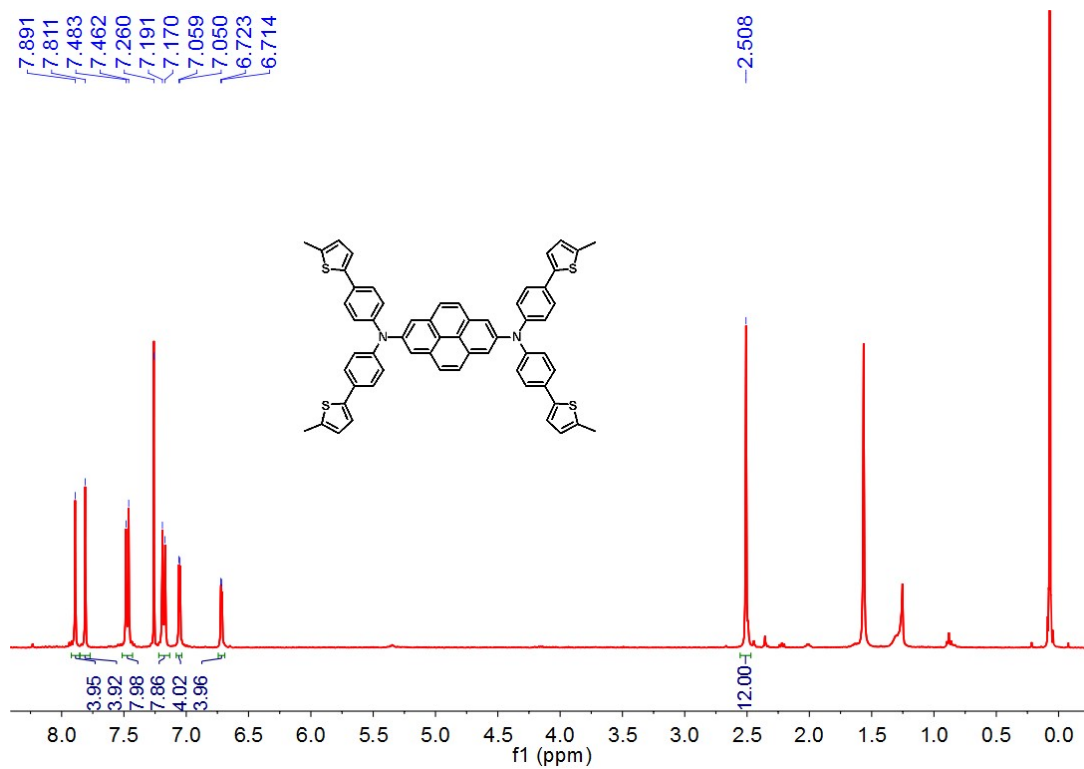


Fig. S6 ¹H NMR of MT2 recorded in CDCl₃.

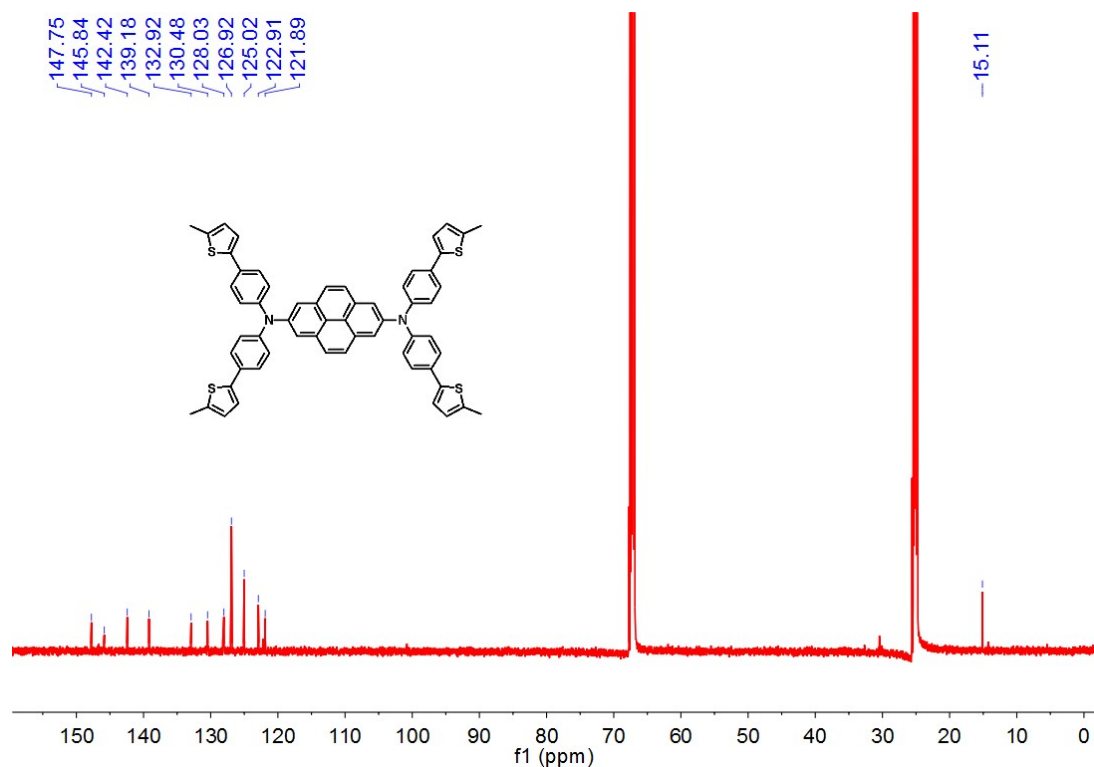


Fig. S7 ^{13}C NMR of MT2 recorded in THF- d_8 .

Elemental Composition Report

Page 1

Single Mass Analysis

Tolerance = 15.0 PPM / DBE: min = -1.5, max = 50.0

Element prediction: Off

Number of isotope peaks used for i-FIT = 3

Monoisotopic Mass, Even Electron Ions

4 formula(e) evaluated with 1 results within limits (up to 50 best isotopic matches for each mass)

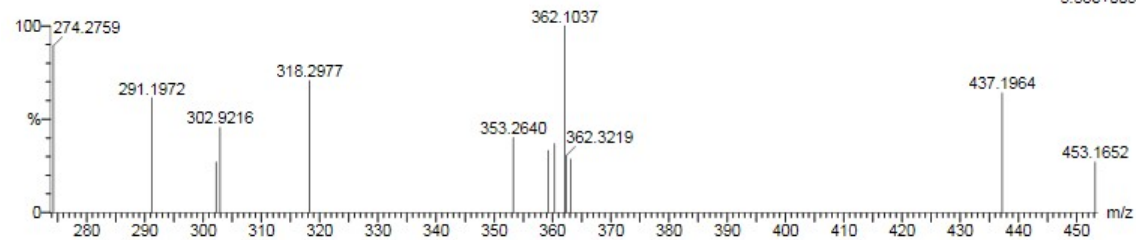
Elements Used:

C: 0-22 H: 0-20 N: 0-1 S: 0-2

WH-ZHU

ZW-ZH-IMS 143 (1.634) Cm (138:145)

1: TOF MS ES+
3.56e+003



Minimum:
Maximum:

5.0 15.0 -1.5
50.0

Mass	Calc. Mass	mDa	PPM	DBE	i-FIT	i-FIT (Norm)	Formula
362.1037	362.1037	0.0	0.0	13.5	38.3	0.0	C22 H20 N S2

Fig. S8 High resolution mass spectrometry of intermediate 5.

Single Mass Analysis

Tolerance = 5.0 PPM / DBE: min = -1.5, max = 50.0

Element prediction: Off

Number of isotope peaks used for i-FIT = 3

Monoisotopic Mass, Even Electron Ions

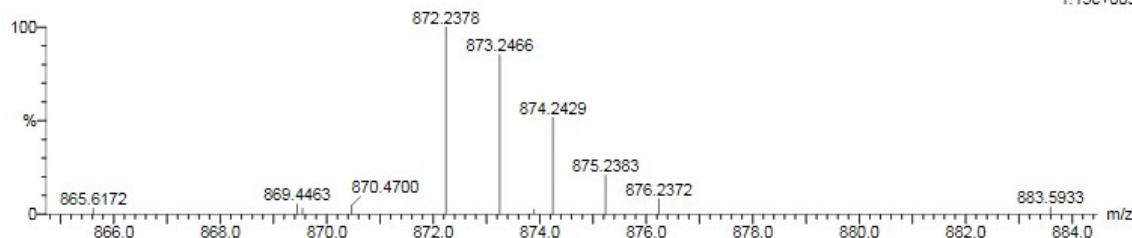
8 formula(e) evaluated with 1 results within limits (up to 50 closest results for each mass)

Elements Used:

C: 0-56 H: 0-45 N: 0-2 S: 0-4

DH-QU

QD-LY-001 73 (0.821) Cm (73.74)

1: TOF MS ES+
1.13e+003

Mass	Calc. Mass	mDa	PPM	DBE	i-FIT	i-FIT (Norm)	Formula
873.2466	873.2466	0.0	0.0	35.5	24.6	0.0	C56 H45 N2 S4

Fig. S9 High resolution mass spectrometry of MT1.

Single Mass Analysis

Tolerance = 10.0 PPM / DBE: min = -1.5, max = 50.0

Element prediction: Off

Number of isotope peaks used for i-FIT = 3

Monoisotopic Mass, Even Electron Ions

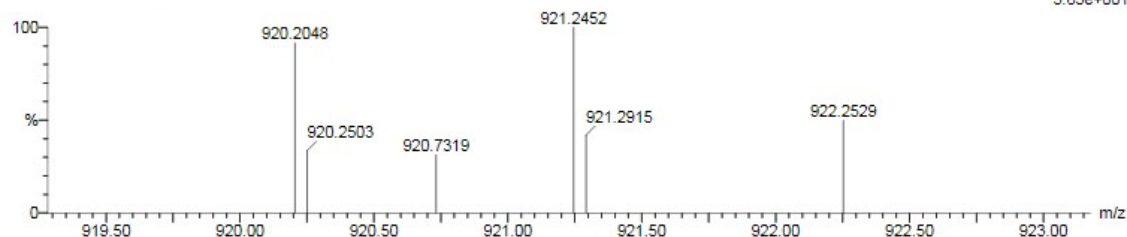
22 formula(e) evaluated with 1 results within limits (up to 50 closest results for each mass)

Elements Used:

C: 0-60 H: 0-99 N: 0-2 S: 0-4

WH-ZHU

ZW-ZH-0425 304 (3.504) Cm (301.311)

1: TOF MS ES+
5.85e+001

Mass	Calc. Mass	mDa	PPM	DBE	i-FIT	i-FIT (Norm)	Formula
921.2452	921.2466	-1.4	-1.5	39.5	23.6	0.0	C60 H45 N2 S4

Fig. S10 High resolution mass spectrometry of MT2.

6. DFT/TDDFT calculation of MT1 and MT2

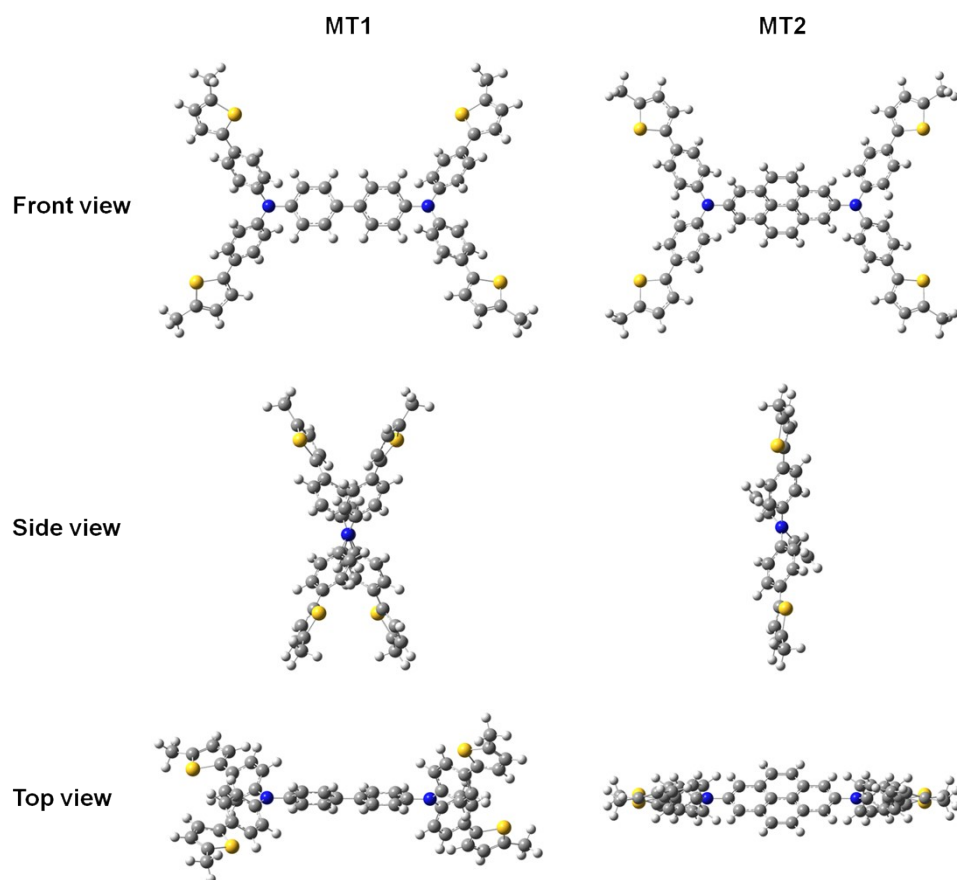


Fig. S11 Optimized geometries of MT1 and MT2.

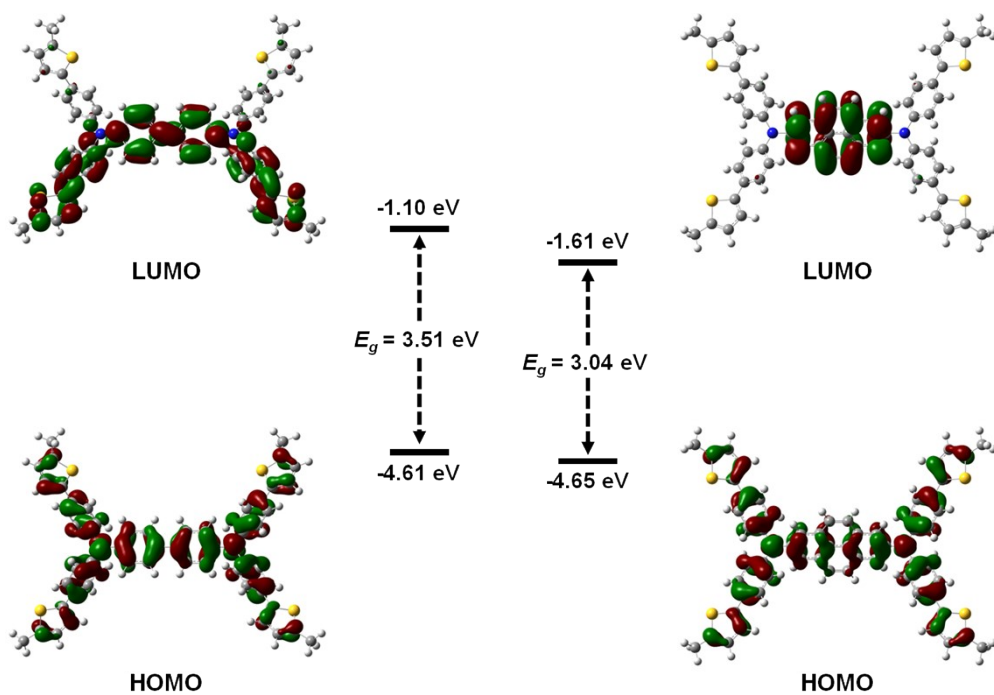


Fig. S12 DFT calculated frontier molecular orbitals for MT1 and MT2.

Table S1. The selected vertical transition energies, wavelengths, oscillator strengths, and excited-state electronic configurations as determined with TDDFT at the B3LYP/6-31G* level of theory.

Compound		E_{vert} (eV)	λ_{vert} (nm)	f	Configuration
MT1	S0→S1	3.0038	412.75	1.4759	HOMO→LUMO (8.4%)
					HOMO→LUMO+1 (54.6%)
					HOMO→LUMO+2 (32.1%)
MT2	S0→S1	2.5828	480.03	0.0300	HOMO→LUMO (97.1%)
	S0→S2	2.8412	436.38	0.0003	HOMO-1→LUMO (98.63%)
	S0→S3	3.0771	402.92	1.3394	HOMO→LUMO+3 (94.5%)

All of the calculations were performed with gaussian 16 package. The B3LYP function and the 6-31G* basis set is selected throughout the calculation. The geometric structures were calculated at DFT/TDDFT level. All the structural optimizations had no restrictions on bonds, angles and dihedral angles. Otherwise, in order to make the calculation results more consistent with the experimental requirements, we considered the solvent dichloromethane based on the polarizable continuum model (PCM) using the integral equation formalism variant (IEFPCM). The S0→S2 transition of MT2 exhibits extremely low oscillator strength, making it difficult to be observed experimentally.

7. Thermal properties of MT1 and MT2

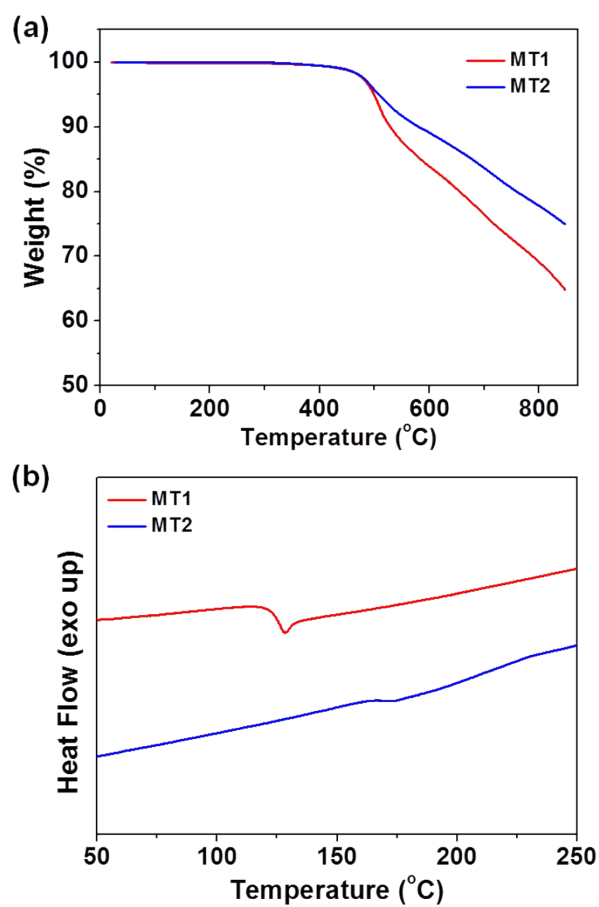


Fig. S13 (a) Thermogravimetric analysis curves recorded for **MT1** and **MT2** under nitrogen at a heating rate of $10\text{ }^{\circ}\text{C min}^{-1}$. (b) The second DSC heating traces of **MT1** and **MT2** previously heated and cooled with a scan rate of $10\text{ }^{\circ}\text{C min}^{-1}$ under a nitrogen atmosphere.

8. XPS, SEM, AFM, PL and TRPL results

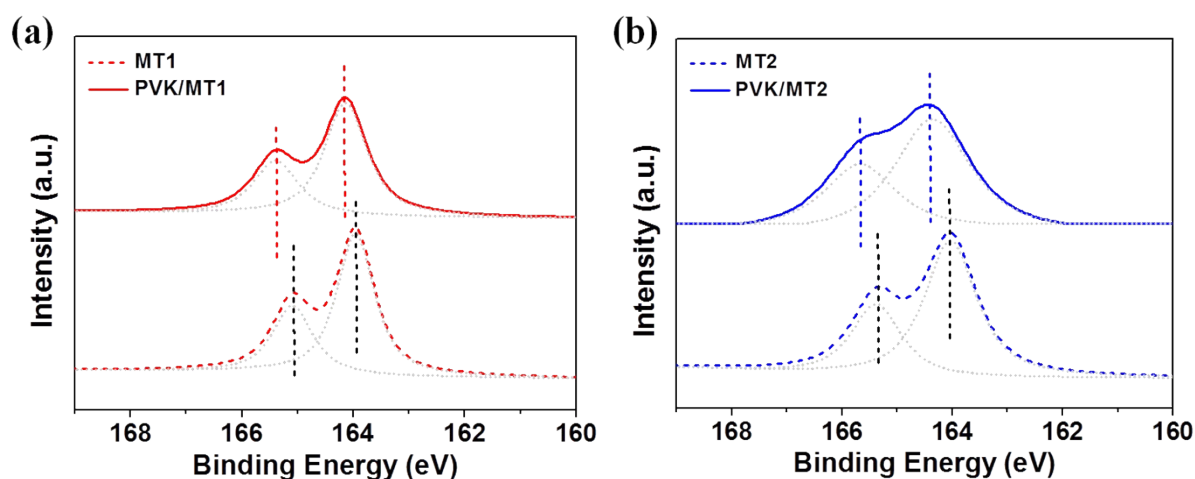


Fig. S14 XPS spectra of the binding energy of S 2p in (a) MT1 and PVK/MT1 film and (b) MT2 and PVK/MT2 film.

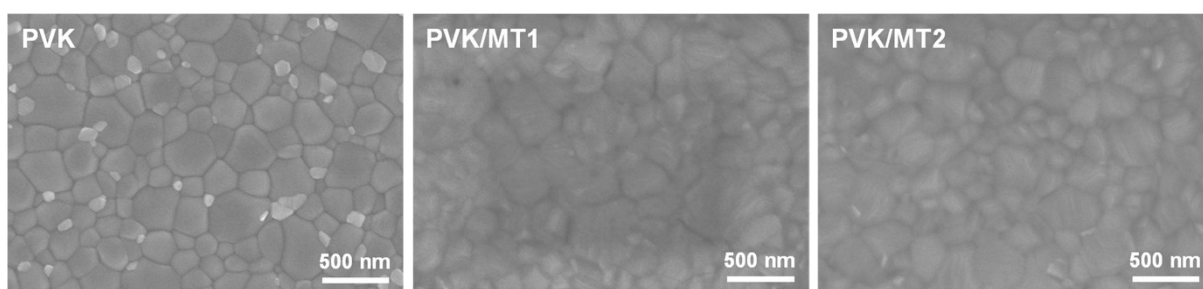


Fig. S15 The top-view SEM images of pristine perovskite film, and perovskite films coated with MT1 and MT2, respectively.

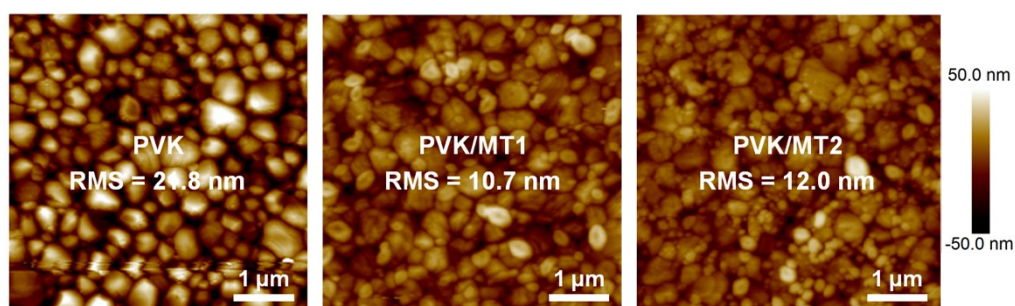


Fig. S16 The AFM images of pristine perovskite film, and perovskite films coated with MT1 and MT2, respectively.

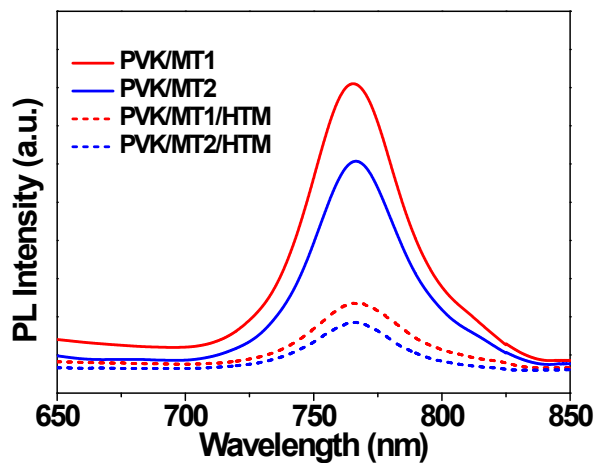


Fig. S17 Steady-state PL spectra of MT1 and MT2 treated perovskite films without/with HTM layer, respectively.

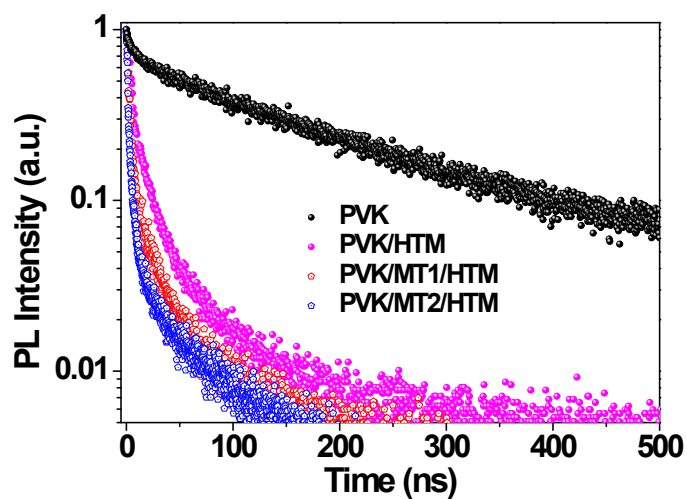


Fig. S18 TRPL spectra of pristine perovskite film, perovskite film with HTM layer, MT1 and MT2 treated perovskite films with HTM layer, respectively.

9. The J - V curve, IPCE spectra and integrated current curves

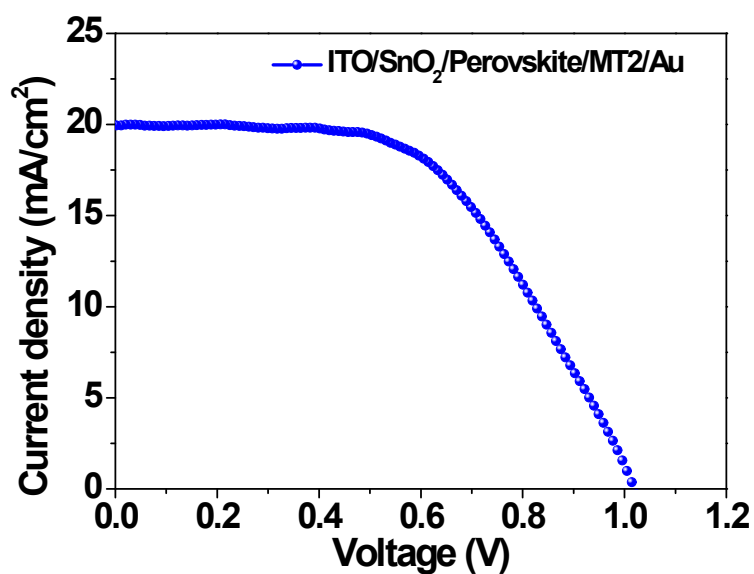


Fig. S19 J - V curve of PSC device with MT2 as the hole transporting layer.

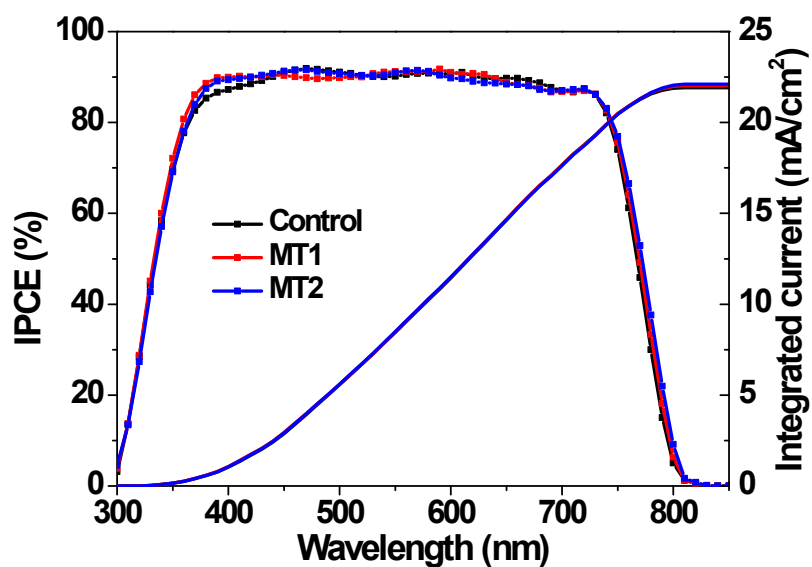


Fig. S20 The IPCE spectra and integrated current curves of the control devices and the devices with different SIMs treatment.

10. The operation stability test at elevated temperature

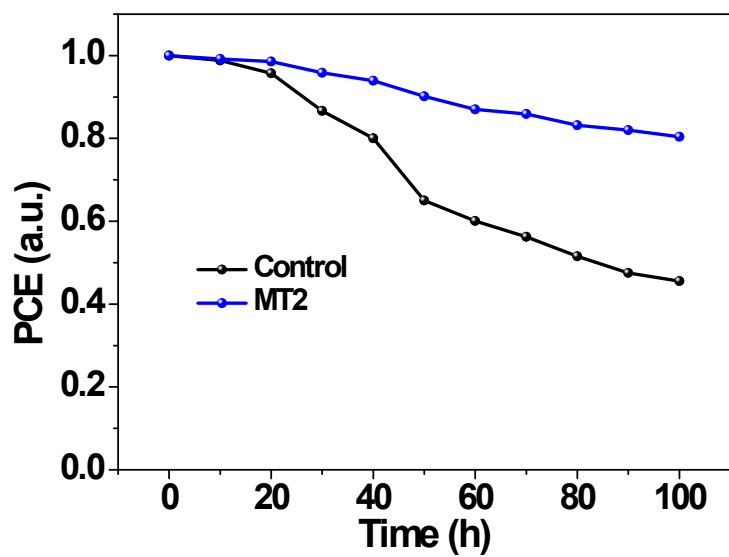


Fig. S21 The operation stability test of the control and MT2 based PSCs under continuous one sun illumination in nitrogen environment at a elevated temperature of 55-60 °C.

11. Time-resolved photoluminescence decay fitting parameters

Table S2. Time-resolved photoluminescence decay fitting parameters of pristine and passivated perovskite film.

Sample	A ₁ (%)	τ_1 (ns)	A ₂ (%)	τ_2 (ns)	τ_{avg} (ns)
PVK	2.26	9.25	97.74	155.02	151.73
PVK/MT1	11.47	7.12	88.53	59.31	53.32
PVK/MT2	10.68	5.99	89.32	54.03	48.90
PVK/Spiro	48.46	5.42	51.54	38.64	22.54
PVK/MT1/Spiro	45.49	2.85	54.51	27.47	16.27
PVK/MT2/Spiro	50.27	1.66	49.73	24.81	13.17

12. Thickness measurement results

Table S3. Thickness measurement results of MT1 and MT2 films deposited on Si substrates.

Sample	Position 1 (nm)	Position 2 (nm)	Position 3 (nm)	Average (nm)
MT1	3.74	3.69	4.45	3.96
MT2	4.99	4.10	3.94	4.34

13. References

1. M. H. Chua, H. Zhou, T. T. Lin, J. Wu and J. W. Xu, *J. Polym. Sci., Part A: Polym. Chem.*, 2017, **55**, 672-681.